Hadronic intermittency and chaotic motion in rapidity space

N. G. Antoniou and F. K. Diakonos
University of Athens, 15771 Athens, Greece

C. G. Papadopoulos
CERN, TH Division, CH-1211, Geneva 23, Switzerland

P. Schmelcher
Institute for Physical Chemistry, INF253, 6900 Heidelberg, Germany

(Received 23 June 1993)

We show that the Hamiltonian dynamics of the effective two-particle potential, describing an additional component of the hadronic S matrix and corresponding to the Feynman-Wilson fluid in one dimension, leads to trapped chaotic and/or diffusive intermittent motion. We argue that the strong density fluctuations in rapidity space, generated by this motion, are related to the intermittency of the multihadron distributions at high energies.

PACS number(s): 05.45.+b, 13.85.Hd, 12.38.Mh

I. INTRODUCTION

In a recent investigation [1] on the nature of intermittency phenomena in high-energy collisions, we have shown that a factorizable, unitary, and self-consistent component of the hadronic S matrix, satisfying, as an additional constraint, self-similarity in rapidity space, leads to a monofractal pattern in multiparticle production processes. This component of the S matrix has the structure of a one-dimensional classical fluid in rapidity space y at a critical temperature $T=T_c$ [critical Feynman-Wilson (FW) fluid]. We have interpreted this nonconventional component of the hadronic density in rapidity space as the signature of states originated by a quark-hadron phase transition at $T=T_c$, in a high-energy collision. We have also argued that in present experiments the bulk of the events belong to the conventional sector of low-transverse-momentum (low-p_T) physics and, therefore, the observed intermittency effect is rather weak because it is masked by the ordinary short-range correlations in rapidity space [2]. In future experiments, however, especially with relativistic heavy ions, one expects to observe strong intermittency patterns with a single fractal dimension ($d_F \simeq 0.7$–0.8) as evidence for a second-order phase transition in a process dominated by quark-gluon plasma formation.

In this work we attempt to connect the fractal structure of the critical FW fluid, reflecting the self-similarity constraint of a particular sector of the S matrix, with the geometrical properties of the Hamiltonian motion of the analog system driven by the corresponding effective potential at $T=T_c$.

The basic equations of the critical FW fluid in the thermodynamic limit, specifying (a) the canonical partition function $Z_c(N,\Delta)$, (b) the effective two-particle potential $V_{\text{eff}}(y-y')$, (c) the density-density correlation function $\langle \rho(y)\rho(y') \rangle$, (d) the intermittent behavior of the factorial moments $F_p(\delta,\Delta)$, and (e) the Mueller propagator $G(y-y')$, are summarized as follows:

$$Z_c(N,\Delta) = \int dy_1 dy_2 \cdots dy_N dp_1 dp_2 \cdots dp_N \exp\left[-\frac{H_{\text{eff}}}{kT_c}\right], \tag{1}$$

$$\frac{H_{\text{eff}}}{kT_c} = \sum_{i=1}^{N} \frac{p_i^2}{2} + \sum_{i=0}^{N} V_{\text{eff}}(y_{i+1}-y_i) \qquad (y_0=0,\ y_{N+1}=\Delta,\ y_{i+1}>y_i), \tag{2}$$

$$V_{\text{eff}}(y-y') = \frac{1+\eta}{2\eta} \ln\left|\frac{y-y'}{\delta_0}\right| + \eta(1-\eta)^{(1-\eta)/\eta}\left|\frac{y-y'}{\delta_0}\right|^{(\eta-1)/\eta}, \tag{3}$$

$$\langle \rho(y)\rho(y') \rangle = Q_c^{-1}(\Delta) \sum_N \int dy_1 dy_2 \cdots dy_N dp_1 dp_2 \times \cdots dp_N \rho(y)\rho(y') \exp\left[-\frac{H_{\text{eff}}}{kT_c}\right], \tag{4}$$

$$\rho(y) = \sum_{i=1}^{N} \delta(y-y_i), \quad Q_c(\Delta) = \sum_N Z_c(N,\Delta), \tag{5}$$

$$F_p(\delta,\Delta) = \frac{p![\Gamma(1-\eta)]^{p-1}}{\Gamma[1+\eta+(1-\eta)p]} \left[\frac{4\delta}{\Delta}\right]^{-\eta(p-1)} \qquad (\delta_0 \ll \delta \ll \Delta), \tag{6}$$

$$G(\omega-\omega') = \frac{\delta_0^{-1}}{2\pi i} \int_{c-i\infty}^{c+i\infty} [\exp(\lambda^{1-\eta})-1]^{-1} e^{\lambda(\omega-\omega')} d\lambda \qquad (\omega = y/\delta_0), \tag{7}$$

$$G(\omega-\omega') \sim |\omega-\omega'|^{-\eta} \quad (|\omega-\omega'| \gg 1). \tag{8}$$

In these equations, describing the one-dimensional physics of a newly hadronized system in rapidity space (at $T=T_c$), Δ is the size of the system, δ_0 is a minimal scale, and η is a critical exponent ($0<\eta<1$) related to the fractal dimension $d_F=1-\eta$. The long-range attraction (logarithmic tail) in the potential (3) allows for a critical behavior of the system, since the absence of long-range forces would prevent the development of a phase transition in one dimension.

In this work we address the question of whether the classical motion of the hadronic chain specified by the Hamiltonian (2), together with the ergodic hypothesis, may reveal important geometrical characteristics which are connected with the origin of the fractal structure of the S matrix in the hadronization sector. In a simplified version of this motion corresponding to the minimal configuration ($N=2$), the nonintegrability of the system is investigated and the generation of nonzero entropy is established. More specifically, in Sec. II the instability of the motion is studied, and the corresponding Liapunov exponents are calculated in order to discriminate regular from chaotic trajectories. In particular, trapped chaotic as well as diffusive intermittent chaotic trajectories with finite Liapunov exponents are found and singled out at relatively low energies. These trajectories generate strong density fluctuations in rapidity space within the ergodic background, i.e., nonlocalized chaotic motion in rapidity space which occurs at high energies. In Sec. III the connection of these trajectories with the fractal structure of the S matrix in rapidity space and the possibility of extending our approach for large N (the thermodynamic limit) are discussed.

II. CLASSICAL HAMILTONIAN DYNAMICS

In the minimal configuration ($N=2$) of the hadronic chain, the corresponding mechanical system reduces to a two-degrees-of-freedom Hamiltonian system with potential energy

$$V(y_1,y_2)=\frac{\eta+1}{2\eta}\left[\ln(x)+\ln(y-x)+\ln(1-y)-3\ln\left[\frac{\delta_0}{\Delta}\right]\right]+\left[\frac{\delta_0}{\Delta}\right]^{(1-\eta)/\eta}[\eta(1-\eta)]^{(1-\eta)/\eta}\left[\frac{1}{x^{(1-\eta)/\eta}}+\frac{1}{(y-x)^{(1-\eta)/\eta}}+\frac{1}{(1-y)^{(1-\eta)/\eta}}\right], \tag{9}$$

where the reduced rapidities $x=y_1/\Delta$ and $y=y_2/\Delta$ are scaled with Δ. The motion is restricted to the $0<y_1<y_2<1$ region of the y_1,y_2 plane. In Fig. 1 the equipotential curves $V(x,y)=$const for some choice of the parameter values η,δ_0 ($\eta=0.5$, $\delta_0=0.2$) are shown. The potential possesses three minima—each lying on a median of the triangle defined by $y=1$, $y=x$, $x=0$ in the x,y plane and having a Euclidean distance $O(\delta_0)$ from the corresponding vertex—and one maximum lying at the barycenter of the triangle ($x=\frac{1}{3}$, $y=\frac{2}{3}$).

The main tools we will use in order to describe the classical motion in the above potential are the Liapunov exponents, as calculated from the equations of motion, and the Toda criterion on the Gaussian curvature of the potential. We adopt the definition of Refs. [3] for the spectrum of Liapunov exponents looking at the long-term evolution of an infinitesimal $2N_F$ sphere of initial conditions (N_F is the number of degrees of freedom for the considered system). After time t, the sphere will be deformed via the equations of motion to a $2N_F$ ellipsoid. The ith one-dimensional Liapunov exponent is then defined as

$$\lambda_i=\lim_{t\to\infty}\frac{1}{t}\log\frac{p_i(t)}{p_i(0)}\ , \tag{10}$$

where $p_i(t)$ is the length of the ellipsoid principal axis and λ_i are ordered from largest to smallest.

In the case of a two-dimensional conservative nonintegrable system, there are two nonvanishing Liapunov exponents of equal magnitude and opposite sign, so that the whole Liapunov spectrum is only determined through the maximal Liapunov exponent. To characterize a system's trajectory as regular ($\lambda_{\max}=0$) or not ($\lambda_{\max}\neq 0$), we also determine its Poincaré section [4], so that we can test the convergence of the limit (10).

Let us now study the motion in the potential (9) for the various values of the total energy

$$E=\frac{p_x^2}{2\Delta^2}+\frac{p_y^2}{2\Delta}+V(x,y)\ . \tag{11}$$

For $x=x_{\min}$ and $y=y_{\min}$ the potential has a minimum

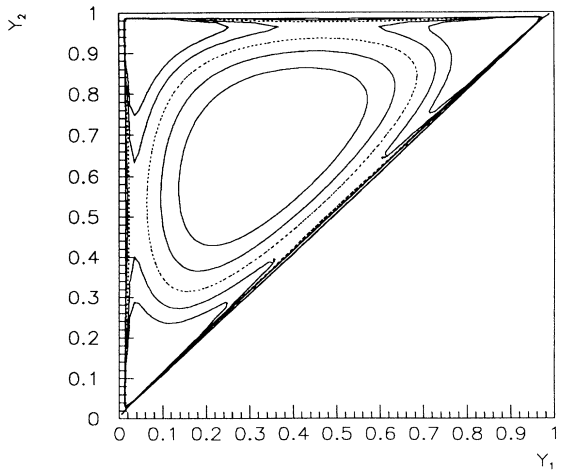

FIG. 1. Potential contours.

$E_{\min}=V(x_{\min},y_{\min})$. The values $x_{\min}$ and $y_{\min}$ are determined numerically for an arbitrary value of the parameters η,δ_0. For $\eta=\frac{1}{2}$, however, one can find an analytic expression in terms of δ_0:

$$x_{\min}=\frac{1}{4}+\frac{\delta_0}{24\Delta}-\frac{1}{4}\left[\left[1+\frac{\delta_0}{6\Delta}\right]^2-\frac{4\delta_0}{3\Delta}\right]^{1/2},$$

$$y_{\min}=2x_{\min}. \quad (12)$$

There are also two other sets of x,y values where $V(x,y)$ has minima equal to $E_{\min}$ which can be found from symmetry considerations. In the following analysis we will restrict ourselves to the special choice of parameters $\eta=0.5$, $\delta_0/\Delta=0.05$, but the situation is no different for any other set of parameters provided that the conditions $0<\eta<1$ and $\delta_0\ll\Delta$ suggested by the hadronic FW-fluid model are fulfilled. For these parameter values the minimum of the potential is $E_{\min}\approx 2.10$. For energies very close to $E_{\min}$, one expects that the motion is regular, the minima of the potential being elliptic fixed points. In order to study this behavior, Toda [5] suggested considering the Gaussian curvature of the potential defined by

$$K(x,y)=\frac{\left[\frac{\partial^2 V}{\partial x^2}\right]\left[\frac{\partial^2 V}{\partial y^2}\right]-\left[\frac{\partial^2 V}{\partial x\,\partial y}\right]^2}{\left[1+\left[\frac{\partial V}{\partial x}\right]^2+\left[\frac{\partial V}{\partial y}\right]^2\right]^2}. \quad (13)$$

One can prove that if $K(x,y)$ is positive in the whole region of the x,y plane, allowing for the system's motion at a given energy, then for that energy value the motion will be regular in the entire phase space [6]. The critical energy, above which regions with negative curvature occur, can be calculated analytically and is $E_c\approx 2.38$. Regular motion, however, dominates for a large energy zone above E_c and only for $E\geq E_{\rm th}\approx 5$ is chaotic motion observably frequent.

The potential has a saddle point at energy $E_s\approx 5.74$, above which the motion is no longer restricted inside the walls of a single minimum but the system can travel between the regions of the three minima. The allowed phase space (the energy shell) is dominated by the chaotic trajectories. Nevertheless, the motion of the system is mainly localized inside the minima of the potential. Finally, the maximum of the potential is at $E_{\max}\approx 8.5$, and above this energy the motion is completely dominated by chaotic trajectories bounded only through the infinite barriers at $x=y$, $x=0$, and $y=1$.

The picture of the potential characteristics given above leads to the following classification of the trajectories of the mechanical system.

(i) For energies $E_{\min}\leq E\leq E_{\rm th}$, the trajectories are regular, i.e., periodic or quasiperiodic, orbits, with vanishing Liapunov exponents [$O(10^{-3})$ for $t=250$]. Using as Poincaré section the (x,y) plane at $p_x+p_y=0$, we can recognize the resulting KAM tori corresponding to these trajectories in consistency with the regularity of the motion [Figs. 2(a) and 2(b)].

(ii) For energies $E_{\rm th}\leq E\leq E_s$, chaotic trajectories with $\lambda_{\max}\neq 0$ appear, which cover a dominant part of the phase space as the energy increases. The motion is restricted inside the walls of a single minimum, and the corresponding Poincaré section consists of (x,y) pairs filling ergodically a substantial part of the energetically allowed region around the minimum, a sign that the Kolmogorov-Arnold-Moser (KAM) tori are broken up [Fig. 3(a)] as a result of a regularity to chaos transition. These trajectories are the trapped chaotic ones and their appearance is essentially due to the fact that the Toda energy E_c is well below the separatrix or saddle-point energy E_s. This might be the result of the existence at the same time of a repulsive hard sphere and of an attractive logarithmic tail in the two-particle interaction, a question deserving further investigation. Notice that the chaotic motion appears inside the minima corresponding to small values of $\delta y=y_2-y_1$, whereas in the third minimum the quasiperiodic structures dominate [Fig. 3(b)]. This is in agreement with the intuitive expectation that hadronic intermittency is shown at small values of δy.

(iii) Another interesting category of trajectories occurs at the energy region $E_s\leq E\leq E_{\max}$. The saddle-point energy E_s can be seen as a kind of separatrix above which the motion is no longer restricted inside the walls of a single minimum but traveling between different minima is allowed. Trajectories with a nonvanishing Liapunov exponent exist, having time intervals where the motion is almost periodic (laminar phases). We call them diffusive intermittent trajectories. Two different time scales ap-

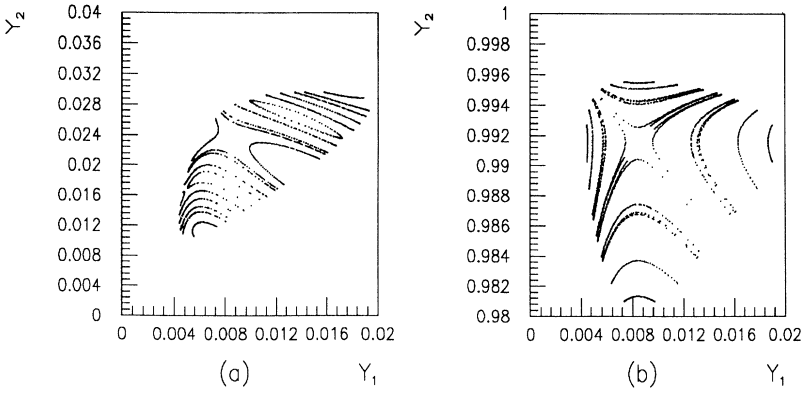

FIG. 2. Poincaré section for $E=2.5$. (a) corresponds to the minimum with $y_1<y_2<0.5$, and (b) to the minimum with $y_1<0.5<y_2$.

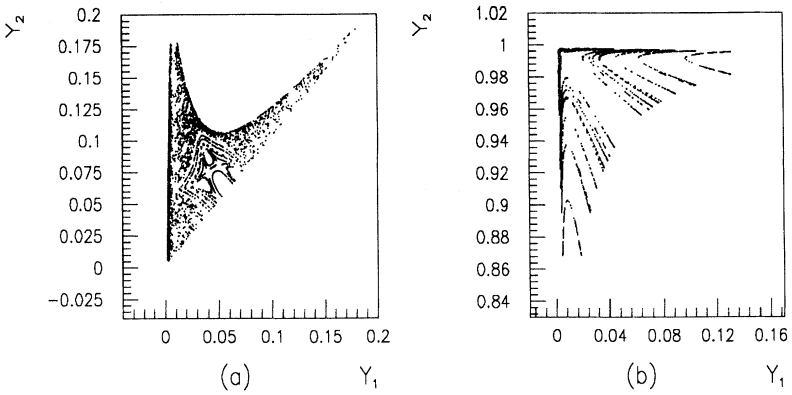

FIG. 3. Poincaré section for $E=5$. (a) corresponds to the minimum with $y_1<y_2<0.5$, and (b) to the minimum with $y_1<0.5<y_2$.

pear in the motion of the system. One scale is connected with the quasiperiodic motion from one minimum to the other, and the second is connected with the chaotic motion inside a single minimum. These two time scales are characteristic for two-dimensional bounded Hamiltonian systems showing intermittency [7]. An example of such an intermittent trajectory is presented in Fig. 4. In Fig. 4(a) the time evolution of the phase space variable $\delta y = y_2 - y_1$ for some choice of initial conditions and for energy $E=6$ is shown. The motion between the two minima (corresponding to $\delta y \approx 0$ and $\delta y \approx 1$) appears to be almost periodic, leading to time intervals with approximately constant (short duration of periodic motion) or even decreasing (long duration of periodic motion) Liapunov functions [Fig. 4(b)]. The chaoticity of this trajectory can be seen in Fig. 4(c) presenting its Poincaré section. Finally, to show the existence of two characteristic time scales in these trajectories, we calculate the corresponding power spectrum presented in Fig. 4(d). One dominant peak is at zero frequency and reflects the chaotic component of the motion following very closely the $1/f^a$ (with $a \approx 1.6$) behavior characteristic of dynamical systems with intermittency, while a second sharp peak at $f_p \approx 0.4$ connected with the intervals of periodic motion is easily recognized.

(iv) The last class of trajectories is for energies $E \geq E_{\max}$ and consists of what we call ergodic background. In this high-energy region almost all the phase space is covered by irregular trajectories with a big maximal Liapunov exponent, and the motion of the system is only restricted by the outer wells of the potential.

After the classification of the different types of trajectories of the Hamiltonian system is made, one has to find out the weight of the irregular relative to the regular trajectories at a given energy shell. Following Ref. [8], we can decompose the energy shell Γ_E into a regular part

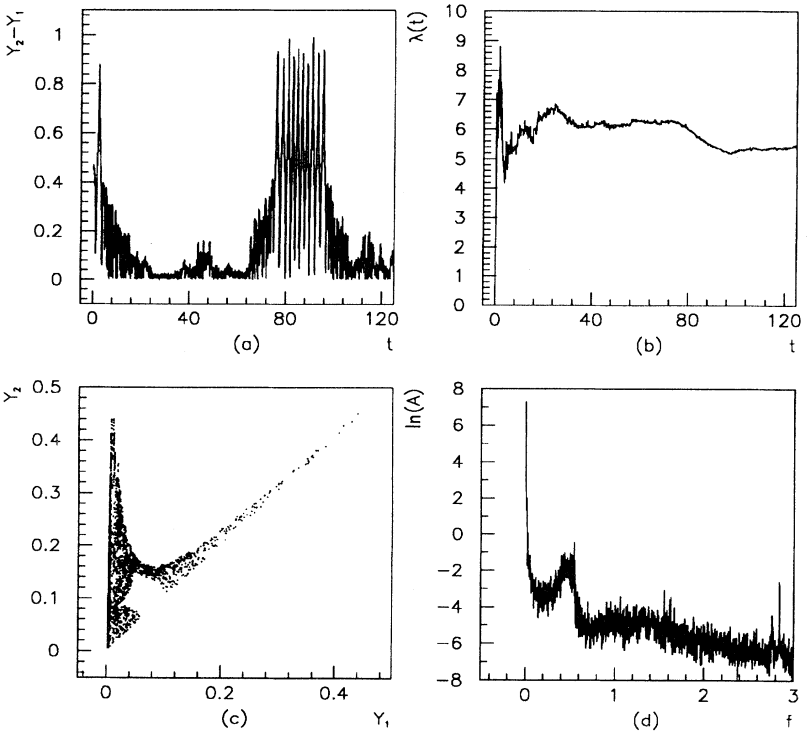

FIG. 4. (a) Relative rapidity δy as a function of time. (b) The Liapunov function. (c) The Poincaré section. (d) The power spectrum.

Γ_E^r and an irregular part Γ_E^i so that $\Gamma_E = \Gamma_E^r \otimes \Gamma_E^i$. To measure the degree of chaos at some energy E, we use the quantity $q(E) = |\Gamma_E^i|/|\Gamma_E|$, where $|A|$ means the volume of A. With the help of the characteristic function

$$X(\gamma) = \begin{cases} 1 & \text{if } \lambda_{\max}(\gamma) > 0 \\ 0 & \text{if } \lambda_{\max}(\gamma) = 0 \end{cases} \tag{14}$$

(γ is the symbol characterizing a trajectory in phase space), we determine $q(E)$ as

$$q(E) = \frac{\int d\gamma\, X(\gamma)\delta(H(\gamma) - E)}{\int d\gamma\, \delta(H(\gamma) - E)} . \tag{15}$$

A nonvanishing $q(E)$ involves a nonvanishing Kolmogorov-Sinai (KS) entropy which can be estimated through

$$K(E) = q(E)\lambda_{\max}^{\text{av}}(E)|\Gamma_E| , \tag{16}$$

where $\lambda_{\max}^{\text{av}}(E)$ is the average of all nonzero Liapunov exponents computed at a particular energy E. To calculate the KS entropy, one has to calculate the Liapunov function over the entire energy shell, a program involving an enormous numerical effort [9]. One can, however, predict the qualitative behavior of the KS entropy as a function of the energy by following the analysis of the motion for the different energies given above. It is expected, therefore, that for energies $E \leq E_{\text{th}}$, the KS entropy is roughly 0, increasing suddenly for $E > E_{\text{th}}$ until $E = E_{\max}$ is reached. Above $E_{\max}$, the behavior of KS entropy is mostly determined by the $\lambda_{\max}^{\text{av}}(E)$. Assuming that $\lambda_{\max}^{\text{av}}(E)$ is a smooth increasing function of the energy, the same is expected to hold also for the KS entropy. As the trapped chaotic and diffusive intermittent motion arises in the energy region $E_{\text{th}} < E < E_{\max}$, we expect that the chaotic measure $q(E)$ for energies around E_s is of $O(1)$, which means that chaotic motion represents the typical behavior of the Hamiltonian system in the above energy interval.

III. ERGODICITY AND FRACTALITY

In order to establish a relation between the Hamiltonian dynamics of the system and the statistical mechanical property of a Feynman-Wilson fluid in one dimension to exhibit fractal structure in rapidity space, we study the phase-space density. This is a function $\rho(p_i, q_i; t)$ defined on the phase space of the system and obeying the usual time-evolution equation

$$\frac{d}{dt}\rho(p_i, q_i; t) = \sum_{i=1}^{N} \left[\frac{\partial H}{\partial p_i}\frac{\partial}{\partial q_i} - \frac{\partial H}{\partial q_i}\frac{\partial}{\partial p_i} \right] \rho(p_i, q_i; t) . \tag{17}$$

On the other hand, ergodicity is usually defined as the equality of time and phase-space averages for large enough time intervals. Let us consider a phase space Γ and phase-space points labeled by

$$\gamma(t) = [q_1(t), \ldots, q_N(t); p_1(t), \ldots, p_N(t)] .$$

The Hamiltonian evolution can be represented as an operator acting on $\gamma(t)$, $\gamma(t) = T(t)\gamma(0)$. Then, if the system is ergodic, one has

$$\lim_{t \to \infty} \frac{1}{t} \int_0^t du\, f(T(u)\gamma) = \int_{S_E} d\sigma\, f(\gamma) \tag{18}$$

for any integrable function f on phase space. S_E is the energy hypersurface, and $d\sigma$ the measure induced on it. For ergodic systems, one can prove [4] that almost every orbit explores almost every point on the energy surface.

The existence for $N \geq 2$ of chaotic trajectories resulting in a nonzero KS entropy for $E \geq E_{\text{th}}$ is, in principle, enough to justify the ergodicity of the motion of our system on these energy surfaces. This is not, of course, ergodicity in the sense of statistical-mechanical notion, since we know that quasiperiodic structures persist at any energy, but is equivalent to the statement that chaotic motion is dominant on the energy surfaces where the KS entropy is not zero, and thus the motion of the system for large time intervals is well approximated by phase-space averages. This is even stronger in the thermodynamic limit $N \to \infty$, where we know that the measure of the regular orbits becomes negligible [10]. Therefore, we study the properties of our system, at $E \geq E_{\text{th}}$, replacing time averages with phase-space averages [Eq. (18)]. To proceed, we choose a phase-space density which is a stationary solution of Eq. (17). It is natural to assume that the time-independent (stationary) solution of Eq. (17) will be given by the Boltzmann distribution $\exp(-H)$, which is a square-integrable solution and in accordance with Eq. (1). Nevertheless, it is worthwhile to notice that using any square-integrable function of the Hamiltonian $F(H)$, instead of $\exp(-H)$, results only in a different normalization of the phase-space density projected on the energy surface. The projection of the Boltzmann distribution on the y_1, y_2 space, which is the rapidity space for the system, can be seen as the rapidity density produced by the motion of the system. This is given by

$$\rho_B(y_1, y_2; E) = \int dp_1 dp_2 \delta(E - H) \exp(-H) , \tag{19}$$

which after integrating over the momenta becomes

$$\rho_B(y_1, y_2; E) = C(E)\Theta(E - V(y_1, y_2)) , \tag{20}$$

which is proportional to the surface in the y_1, y_2 space allowed for the system. $C(E)$ is a constant depending on the energy. As we have already noticed, chaotic trajectories tend to cover uniformly most of the allowed space in the (y_1, y_2) sections, as is evident from Figs. 2(c) and 3(c). This eventually leads to a constant, nonzero projection of the phase-space density on the allowed y_1, y_2 space, in agreement with Eq. (20).

The fractal structure in rapidity space of the hadronic S matrix reflects the existence of strong fluctuations of the phase-space density generated by the Hamiltonian evolution of the two-particle system. The approximation of replacing the phase-space density by the Boltzmann distribution $\exp(-H)$ enables us to calculate several properties of the Hamiltonian dynamics of this system. For instance, we calculate the factorial moment C_2 of

$\rho_B(y_1,y_2;E)$, in the regime $E \simeq E_s$. This is a measure of the fluctuations generated by the motion of the two-particle system, which are strong in the energy regime around E_s. Using the definition given in [11], we have for the two-dimensional distribution

$$C_2 = \frac{1}{M^2} \sum_{i=1}^{M-1} \sum_{j=i+1}^{M} H[y_1(i),y_2(j)]^2 , \tag{21}$$

with

$$H[y_1(i),y_2(j)] = M^2 \int_{y_1(i-1)}^{y_1(i)} \int_{y_2(j-1)}^{y_2(j)} dy_1 dy_2 \rho_B(y_1,y_2;E) , \tag{22}$$

where $y_1(i)=i/M$, $y_2(j)=j/M$, $i,j=0,\ldots,M$. The results of the calculation are shown in Fig. 5(a) as a function of $\ln(M^2)$ and the exponent in the linear fit is $d_2 \approx 0.25$, which is in qualitative agreement with the exponent $d_1=0.5 \approx 2d_2$ calculated using the statistical-mechanical description of the Feynman-Wilson fluid in one dimension. Moreover, the effect of intermittency breaking, i.e., the breaking of the linear behavior of C_2 with respect to $\ln(M^2)$ for distances smaller than $O(\delta_0)$, is evident.

Two remarks are in order. First, the structure of the density $\rho_B(y_1,y_2;E)$ depends only on the characteristics of the potential and not on the normalization we choose, i.e., what solution of Eq. (17) we take. It is proportional to the surface, in the space y_1,y_2, allowed for the system which depends only on the form of the two-particle potential. Furthermore, the property of this interaction to generate trapped chaotic motion with nonzero KS entropy at moderate energies, $E \simeq E_s$, justifies the use of the phase-space averages on the ground of the ergodic hypothesis. Second, the existence of fluctuations in y_1,y_2 space is necessary but not sufficient in order to have a fractal structure. This can be easily verified by calculating the C_2 moment [see Fig. 5(b)] for a density which is nonzero on three cycles with centers lying on (0.1,0.2),(0.1,0.9),(0.8,0.9) in y_1,y_2 space and with radius $r=0.1$. This means that the two-particle potential leads to a specific structure of fluctuations in rapidity space, which can be characterized as self-similar.

In order to study the N-particle potential, for $\eta=0.5$, we calculate the extrema of the potential. Consider the single-particle potential

$$V(x) = \ln\left[\frac{x}{\delta_0}\right] + \frac{\delta_0}{x} \tag{23}$$

and the N-particle one

$$U(x_1,x_2,\ldots,x_n) = \sum_{i=1}^{i=N+1} V(x_i - x_{i-1}) , \tag{24}$$

with $x_0=0$, $x_{N+1}=1$, where we have omitted irrelevant normalization factors. The extrema of the N-particle potential correspond to the configuration where all the distances between the particles can be divided in two groups, $N+1-k$ of them being equal to z_k, where

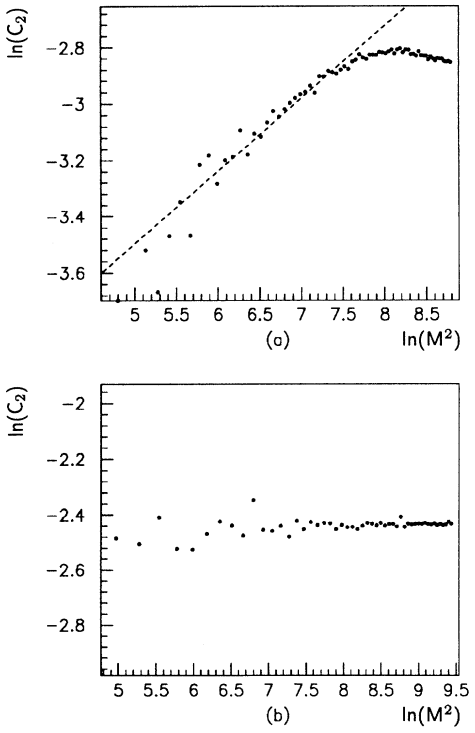

FIG. 5. (a) The $\ln(C_2)$ as a function of $\ln(M^2)$. The dashed line corresponds to $\ln(C_2) \approx 0.25 \ln(M^2) - 4.7$. (b) The $\ln(C_2)$ for a density with nonfractal fluctuations, as explained in the text.

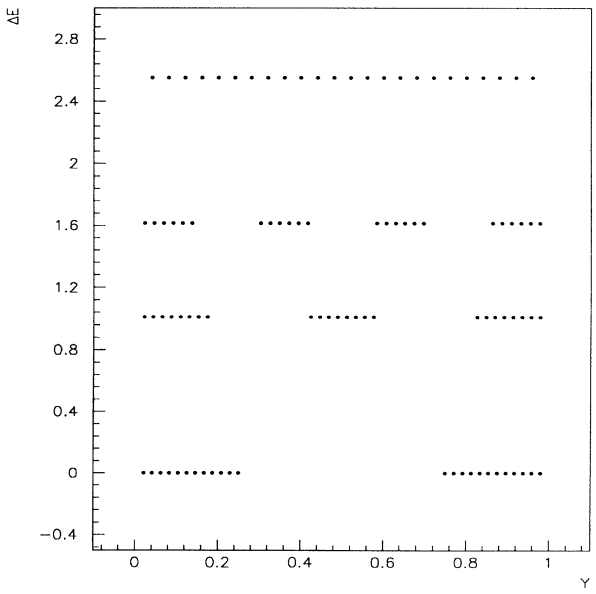

FIG. 6. The energy of the extrema of the potential and their rapidity configurations for $N=24$, as explained in the text.

$$z_k = \frac{1+\delta_0(N+1-2k) \pm \sqrt{[1+\delta_0(N+1-2k)]^2 - 4\delta_0(N+1-k)}}{2(N+1-k)} , \tag{25}$$

and k of them being equal to $[1-(N+1-k)z_k]/k$. The corresponding energy is easily calculated and we find that the minimum energy configuration corresponds to the case $k=1$, whereas the configuration of equidistance particles corresponds actually to the local maximum of the potential, as in the case of the two-particle potential. In Fig. 6 we show the $N=24$ case with $\delta_0=0.02$. Therefore, around the minimum the motion can be approximated by a two-particle potential analogous to Eq. (9) with a minimal scale of $O(N\delta_0)$. Of course, a complete study of the N-particle potential is needed in order to establish the existence of trapped chaotic trajectories around the minimum configuration as well as the existence of diffusive intermittent trajectories visiting different local minimum configurations. Nevertheless, it is hard to believe that this is not the case for large N, since we know that the relative measure of the chaotic region approaches its maximum value 1 when the number of degrees of freedom increases [10].

Therefore, we propose that the fractal properties of the Feynman-Wilson fluid are the result of (a) the nontrivial property of the two-particle potential to generate, in the Hamiltonian motion of the system, trapped and/or diffusive intermittent chaotic trajectories, leading to strong phase-space density fluctuations with fractal structure in rapidity space, and (b) the factorizability of the N-particle potential, leading to a self-similar structure (which is also connected to the Kadanoff scaling), which combined with the clustering property of the potential, gives rise to the assumption that the motion of the N-particle system is qualitatively similar to the two-particle one.

So far, we are considering the hadronic intermittency to be the result of hadron-hadron interactions, assumed to be described at the critical temperature T_c, by the new component of the hadronic S matrix presented in the Introduction. It is expected that above the critical temperature $T > T_c$, the system will be described by the SU(3) gauge theory of strong interactions. At the classical level this theory is believed to exhibit chaotic motion [12]. In the light of our analysis, it is of great interest to investigate in detail the chaotic properties of non-Abelian gauge theories and especially the phase-space density of the quark-gluon system produced in high-energy collisions.

We conclude that it is possible to see the main characteristics of the hadronic intermittency, as described in the framework of the S-matrix model of Ref. [1], in the Hamiltonian dynamics of a simple two-particle potential, on the basis of its property to generate trapped chaotic motion. This combined with the factorizability of the S-matrix model, which is responsible for the self-similarity and the Kadanoff scaling at the critical temperature, can in principle explain the intermittency shown in the multiparticle densities in rapidity space.

ACKNOWLEDGMENTS

We thank H.-D. Meyer for helpful discussions. C.G.P. is partially supported by EEC Program SC1-CT91-0729.

[1] N. G. Antoniou, A. P. Contogouris, C. G. Papadopoulos, and S. D. P. Vlassopulos, Phys. Rev. D **45**, 4034 (1992).

[2] N. G. Antoniou, E. N. Argyres, C. G. Papadopoulos, and S. D. P. Vlassopulos, Phys. Lett. B **260**, 199 (1991).

[3] A. Wolf, J. B. Swift, H. L. Swinney, and J. A. Vastano, Physica D **16**, 285 (1985); I. Shimada and T. Nagashima, Prog. Theor. Phys. **61**, 1605.

[4] M. V. Berry, *Regular and Irregular Motion,* Proceedings of the Workshop on Topics in Nonlinear Dynamics, edited by S. Jorna, AIP Conf. Proc. No. 46 (AIP, New York, 1978), pp. 16–120; O. Bohigas and M. Giannoni, in *Mathematical and Computational Methods in Nuclear Physics,* Lecture Notes in Physics Vol. 209 (Springer, New York, 1984), pp. 1–99.

[5] M. Toda, Phys. Lett. A **48**, 5 (1974)

[6] A. I. Akhiezer, V. I. Truten, and N. F. Shul'ga, Phys. Rep. **203**, 298 (1991).

[7] G. Stolovitzky and J. A. Hernando, Phys. Rev. A **43**, 2774 (1991).

[8] H.-D. Meyer, J. Chem. Phys. **84**, 3147 (1986).

[9] G. Benettin, L. Galgani, and J. Strelcyn, Phys. Rev. A **14**, 2338 (1976).

[10] G. Benettin, C. Froeschle, and J. P. Scheidecker, Phys. Rev. A **19**, 2454 (1979).

[11] A. Bialas and R. Peschanski, Nucl. Phys. **B273**, 703 (1986).

[12] G. K. Savidy, Phys. Lett. B **130**, 303 (1983); T. Kawabe and S. Ohta, Phys. Rev. D **44**, 1274 (1991); B. Müller and A. Trayanov, Phys. Rev. Lett. **68**, 3387 (1992).